Bioorganic & Medicinal Chemistry 19 (2011) 3372–3377

Contents lists available at ScienceDirect

Bioorganic & Medicinal Chemistry

journal homepage: www.elsevier.com/locate/bmc

The square conformation of phenylglycine-incorporated ascidiacyclamide is stabilized by CH/π interactions between amino acid side chains

Akiko Asano *, Takeshi Yamada, Mitsunobu Doi

Osaka University of Pharmaceutical Sciences, 4-20-1, Nasahara, Takatsuki, Osaka 569–1094, Japan

ARTICLE INFO

Article history:
Received 22 March 2011
Revised 14 April 2011
Accepted 18 April 2011
Available online 22 April 2011

ABSTRACT

We designed a phenylglycine (Phg)-incorporated ascidiacyclamide (ASC) analogue, cyclo(-Phg-oxazoline-D-Val-thiazole-Ile-oxazoline-D-Val-thiazole- ([Phg]ASC), with the aim of stabilizing the square conformation of ASC through interactions between amino acid side chains. X-ray diffraction analysis showed that [Phg]ASC has a square structure, similar to ASC, in which the *sec*-butyl group of Ile and the benzene ring of Phg are in close proximity. Consistent with that finding, ^{1}H NMR experiments revealed significant high-field shifts in the *sec*-butyl group of Ile, which suggests a potential for CH/π interactions between the *sec*-butyl group of Ile and the benzene ring of Phg. The CD spectra of [Phg]ASC were less affected by TFE titration or increasing temperature than those of ASC. In addition, [Phg]ASC showed approximately three times greater toxicity toward HL-60 cells than ASC. Thus the potently cytotoxic conformation of [Phg]ASC may be stabilized by CH/π interactions between the side chains of the Ile and Phg residues.

1. Introduction

Ascidiacyclamide, cyclo(-Ile1-Oxz2-D-Val3-Thz4-Ile5-Oxz6-D-Val7-Thz8-) (ASC), is a cytotoxic cyclic octapeptide isolated from tunicate that contains the unusual amino acids oxazoline (Oxz) and thiazole (Thz) (Fig. 1).[1] Studies of the relationship between its structure and symmetry showed that repetition of a four-residue sequence induces C_2-symmetry in the molecule. In addition, introduction of asymmetric modifications in which Ile1 was replaced with other amino acids revealed that ASC and its analogues can assume both square and folded structures,[2–6] and that substitution of an amino acid that disturbs the C_2-symmetry affects the ASC structure.[7–10] Incorporation of an amino acid having the appropriate size results in a square structure and strong cytotoxicity, whereas smaller or larger amino acids induce molecular folding and low cytotoxicity.

In the present study, we endeavored to use the interactions between amino acid side chains to stabilize the square form. We focused on the locations of the side chains of Ile1 and Ile5, which are situated close to one another within the crystal structure of ASC in the square form, and examined the CH/π interactions induced by replacing Ile1 with an aromatic amino acid. We selected phenylglycine (Phg) as the aromatic amino acid because, unlike Phe, Phg does not have a methylene group linked to the aromatic ring. We then synthesized the Phg-containing ASC analogue cyclo (-Phg1-Oxz2-D-Val3-Thz4-Ile5-Oxz6-D-Val7-Thz8-) ([Phg]ASC; Figure 1), and here we describe its characterization using X-ray diffraction, ^{1}H NMR and circular dichroism (CD) spectroscopy.

2. Materials and methods

2.1. Peptide

The ASC analogue [Phg]ASC was synthesized as described previously[11,12] using the conventional liquid-phase method with 1-hydroxy-benzotriazole and 1-ethyl-3-(3-dimethylaminopropyl) carbodiimide hydrochloride (Watanabe Chemical Ind. Ltd.). The replacement of the amino acid at position 1 had no effect on the overall strategy or yield.

[Phg]ASC: ^{1}H NMR (500 MHz, CD_3CN) 293 K δ 0.18 (d, J = 7.0 Hz, 3H, Ile (Cγ2H)$_3$), 0.37 (t, d = 7.0 Hz, 3H, Ile CδH), 0.68 (m, 1H, Ile Cγ1H), 0.98 (m, 1H, Ile Cγ1H), 0.96 (d, J = 6.5 Hz, 3H, D-Val CγH), 0.98 (d, J = 7.0 Hz, 3H, D-Val CγH), 1.12 (d, J = 7.0 Hz, 3H, D-Val CγH), 1.15 (d, J = 6.5 Hz, 3H, D-Val CγH), 1.34 (d, J = 6.5 Hz, 3H, Oxz CγH), 1.42 (d, J = 6.5 Hz, 3H, Oxz CγH), 1.45 (m, 1H, Ile CβH), 2.32 (oct. J = 6.5 Hz, 2H, D-Val CβH ×2), 4.24 (dd, J = 6.5, 1.5 Hz, 1H, Oxz CαH), 4.39 (dd, J = 6.0, 2.0 Hz, 1H, Oxz CαH), 4.68 (m, 3H, Ile CαH, Oxz CβH ×2), 5.09 (dd, J = 10.0, 7.0 Hz, 1H, D-Val CαH), 5.20 (dd, J = 10.0, 6.5 Hz, 1H, D-Val CαH), 5.80 (dd, J = 8.0, 1.5 Hz, 1H, Phg CαH), 7.04 (m, 2H, Phg ArH), 7.18 (m, 3H, Phg ArH), 7.31 (d, J = 10.0 Hz, 1H, D-Val NH), 7.57 (d, J = 10.0 Hz, 1H, D-Val NH), 7.98 (s, 1H, Thz H), 8.09 (d, J = 8.5 Hz, 1H, Ile NH), 8.12 (s, 1H, Thz H), 8.55 (d, J = 8.0 Hz, 1H, Phg NH).

* Corresponding author. Tel.: +81 72 690 1066; fax: +81 72 690 1005.
E-mail address: asano@gly.oups.ac.jp (A. Asano).

0968-0896/$ - see front matter © 2011 Elsevier Ltd. All rights reserved.
doi:10.1016/j.bmc.2011.04.036

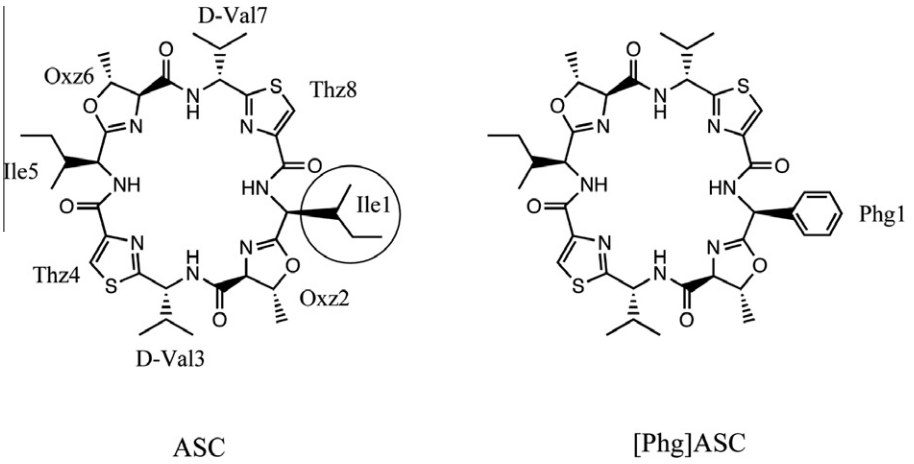

Figure 1. Chemical structures of ASC, [Phg]ASC and [Phe]ASC.

2.2. X-ray diffraction

Crystals of [Phg]ASC were grown from THF–water (Form **I**) and DMF–water (Form **II**) solutions. Form **I**: $C_{38}H_{48}N_8O_6S_2{\cdot}C_4H_8O{\cdot}H_2O$, Mr = 845.1, monoclinic, $C2$, a = 15.844(4) Å, b = 12.750(3) Å, c = 12.957(3) Å, β = 99.945(4)°, V = 2578(1) Å^3, Z = 2, T = 240 K, D_X = 1.117 g cm^{-3}, F(0 0 0) = 924, μ(Mo Kα) = 0.155 mm^{-1}, No. of reflections (obs.) = 9386, θ_{max} = 23.3°, R_{INT} = 0.0289, No. of reflections ($I > 2\sigma(I)$) = 2804, R = 0.0877, wR = 0.2194, $(\Delta/\sigma)_{max}$ = 0.006, $\Delta\rho_{max}$ = 0.701 e Å^{-3}, $\Delta\rho_{max}$ = –0.316 e Å^{-3} (CCDC 809195). Form **II**: $C_{38}H_{48}N_8O_6S_2{\cdot}2(C_3H_7NO)$, Mr = 868.3, monoclinic, C_2, a = 16.313(3) Å, b = 12.299(2) Å, c = 13.022(2) Å, β = 103.279(2)°, V = 2542.6(8) Å^3, Z = 2, T = 200 K, D_X = 1.206 g cm^{-3}, F(0 0 0) = 984, μ(Mo Kα) = 0.162 mm^{-1}, No. of reflections (obs.) = 11701, θ_{max} = 25.7°, R_{INT} = 0.0258, No. of reflections ($I > 2\sigma(I)$) = 3655, R = 0.0782, wR = 0.1456, $(\Delta/\sigma)_{max}$ = 0.008, $\Delta\rho_{max}$ = 0.359 e Å^{-3}, $\Delta\rho_{max}$ = – 0.295 e Å^{-3} (CCDC 809196). The structures were solved using SHELXS-97 and refined using SHELXL-97. In both crystal forms, the crystallographic two-fold axis (*b*-axis) was located on the peptide molecules, and the asymmetric content was half of the peptide molecule. Therefore, the side chains of the Phg and Ile residues were refined in a disordered state with a site occupancy of 0.5. The square structures of Forms **I** and **II** were similar to one another, and the structure of only Form **I** is shown in Figure 3.

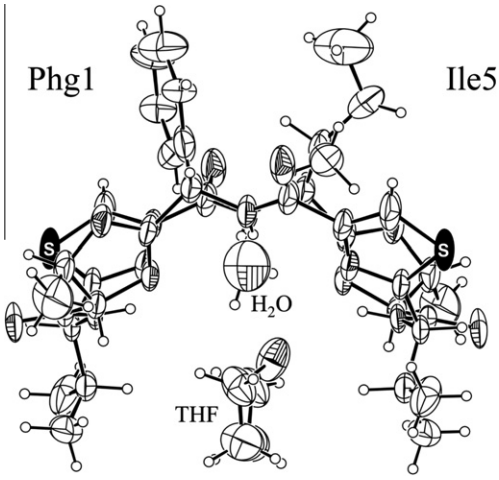

Figure 2. The molecular structure for Form **I** of [Phg]ASC. The crystal structure is disordered by the *b*-axis located on the molecule, and the duplicate moieties of the asymmetric unit are drawn to show the whole peptide structure.

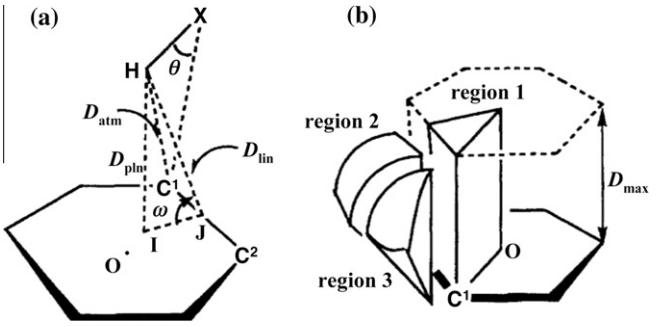

Figure 3. Method for surveying CH/π contacts in a six-membered π-system.[11] (a) O: center of the plane. C^1 and C^2: nearest and second nearest sp^2-carbons to H. ω: dihedral angle defined by the C^1OC^2 and HC^1C^2 planes. θ: $\angle HXC^1$. D_{pln}: H/π-plane distance (H/I). D_{atm}: interatomic distance (H/C^1). D_{lin}: distance between H and line C^1C^2 (H/J). (b) **1**: region where H is above the aromatic ring. **2** and **3**: regions where H is outside region **1** but may interact with the π-orbitals. $D_{pln} < D_{max}$, $\theta < 60$, $|\omega| < 90$ for region 1; $D_{lin} > D_{max}$, $\theta < 60$, $90 < |\omega| < 130$for region 2, and $D_{atm} < D_{max}$, $\theta < 60$, $50 < \phi < 90$ for region 3 (ϕ: HC1I). (θ should be smaller than 60 to avoid contact of atom X with C^1). D_{max}: cutoff value in every region.

2.3. ^{1}H NMR measurement

^{1}H NMR spectra were recorded on a Varian Unity Inova 500 MHz FT NMR spectrometer. Peptide concentrations were ca. 5.0 mM in deuterated acetonitrile (CD_3CN). Chemical shifts were measured relative to internal trimethylsilane at 0.00 ppm. The protons were assigned using two-dimensional correlated spectroscopy (2D-COSY) and rotating Overhauser effect spectroscopy (ROESY; mixing time = 400 ms).

2.4. CD spectra measurement

The CD spectra of ASC and [Phg]ASC were measured using a JASCO 500 A (JASCO, Tokyo, Japan) dichrograph. The peptide concentrations were ca. 0.5 mM, and the path length was 1 cm. Spectra were scanned at 5 nm/min with a 0.1 nm interval for uptake to a computer. Data were averaged for each 1.0 nm and plotted.

2.5. Cytotoxicity measurement

The cytotoxicity of [Phg]ASC was evaluated for P388 lymphocytic leukemia cells and HL-60 human myeloblastic leukemia cells as described previously with some modifications.[13,14] The P388 cells were cultured at 37 °C in Eagle's minimum essential medium

(Nissui) supplemented with 10% fetal calf serum (Gibco). The peptides were dissolved in dimethyl sulfoxide, after which the solution was diluted with medium to give concentrations of 200, 20 and 2 mg/mL. Each solution was then mixed with cells suspended in medium (2 x 10^5 cells/mL). After incubation at 37 °C for 72 h under a 95% air/5% CO_2 atmosphere, the cells were labeled with 5 mg/mL 3-(4, 5-dimethyl-2-thiazoyl)-2, 5-diphenyl-2H-tetrazolium bromide, and absorbance of formazan was measured at 540 nm using a microplate reader (Model 450, BIO–RAD). All assays were performed three times, and the ED_{50} was determined from the semi-logarithmic plots.

3. Results and Discussion

3.1. X-ray diffraction structure

X-ray analysis of the two crystal forms (Form **I** and **II**) of [Phg]ASC revealed two similar square structures that were also similar to those of ASC and its analogues.[2,7,10] The structure of Form **I** is shown in Figure 2. A solvated water and a tetrahydrofuran (THF) molecule are located on the peptide molecule. Within this structure, the respective side chains of Phg1 and Ile5, a benzene group and a *sec*-butyl group, faced each other as is seen with ASC and its analogues.[2,7,10] The nearest distance between the side chains of Phg1 and Ile5 was estimated by surveying the CH/π contacts for the six-membered π-system shown in Figure 3.[15] To participate in a CH/π interaction, the hydrogen atom should be positioned above the π-plane, since the interaction primarily originates from transfer of π-electrons to the antibonding orbital of the C-H bond.[16–20] This, however, does not mean that the hydrogen must lie exactly above the aromatic ring. Thus a C-H hydrogen is able to interact with the π-orbital in regions **2** and **3** in Figure 3 (b), where the hydrogen atom is above the π-plane but slightly offset outside the ring. The distance from H to the π-plane, the distance between H and line C^1-C^2 and the H/C^1 interatomic distance are defined as D_{pln}, D_{lin}, and D_{atm}, respectively. These distance parameters (D_{pln}, D_{lin}, D_{atm}) correspond to regions **1**, **2** and **3**, respectively, in Figure 3 (a). The dihedral angle determined by the π-plane, plane H-C^1-C^2 and angle ∠H-X-C^1 (X = C, O, etc.) are defined as ω and θ, respectively, in Figure 3 (a). An unbonded atomic contact within the [Phg]ASC crystal structure was sought

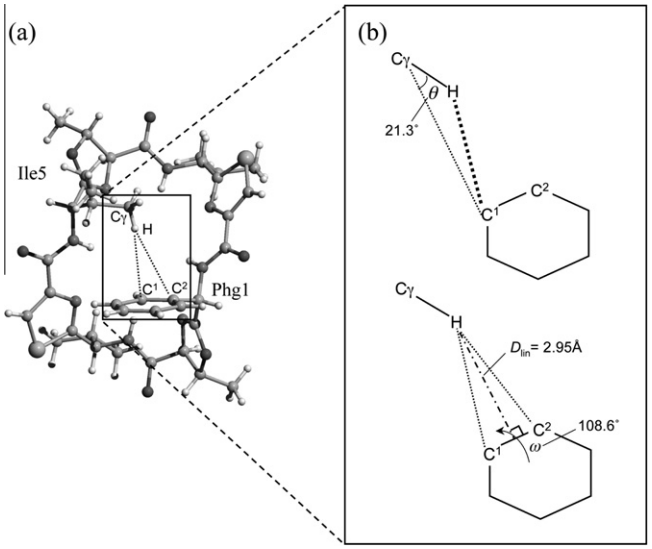

Figure 4. Spatial relationship between Phg1 and Ile5. (a) Overall structure of [Phg]ASC. (b) Expanded schematic views. The distance (D_{lin}) and angle (θ and ω) parameters determined using the method of surveying CH/π contacts in a six-membered π-system are indicated.

between a CH (γCH_3-Ile5) and an aromatic π(C_{sp2}) atom (Phg1) with appropriate distance (D_{lin}) and angle parameters (θ and ω). Figure 4 shows the result of our survey for each value. The angles θ and ω are 21.3° and 108.6°, respectively, indicating γCH_3-Ile5 is located above region **2** of the π-orbital. On the other hand, the CH/π distance (D_{lin}) gives an estimation of 2.95 Å, which is very similar to the sum of the van der Waals radii of H and C_{sp2} (ca. 2.90 Å: ca. 1.20 Å for C–H and ca. 1.70 Å for a half thickness of the aromatic molecule[21,22]). This distance makes it worth considering the presence of CH/π interactions between the side chains of Phg1 and Ile5.

3.2. ^{1}H NMR measurement

^{1}H NMR spectroscopic analysis revealed interactions between methyl and benzene groups based on ring-current effects of the benzene ring, which result in significant high-field shifts of the

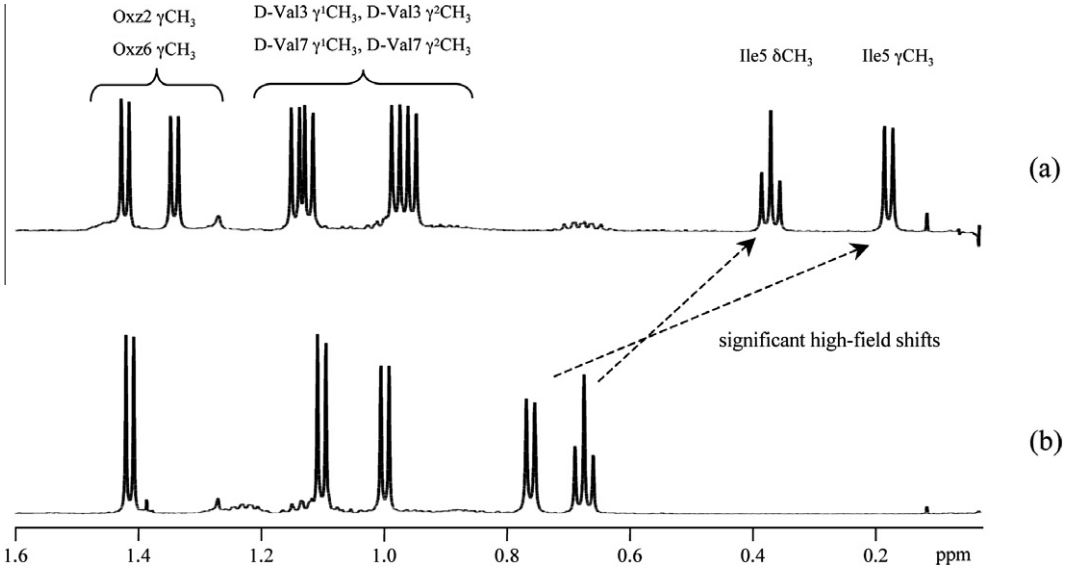

Figure 5. High field portions of the ^{1}H NMR spectra for [Phg]ASC (a) and ASC (b) in CD_3CN. The ^{1}H NMR spectrum of ASC is consistent with either symmetry of the molecule: -Ile1-Oxz2-D-Val3-Thz4- or-Ile5-Oxz6-D-Val7-Thz8-. As the result of this symmetry, equivalent nuclei show the same chemical shift.

Table 1
Chemical shifts (d_{CH3}) and Dd_{CH3} (=$\delta_{CH3(ASC)}-\delta_{CH3([Phg]ASC)}$) values for all CH_3 proton signals included in ASC and [Phg]ASC molecules

		$\delta_{CH3(ASC)}$ (ppm)	$\delta_{CH3([Phg]ASC)}$ (ppm)	$\Delta\delta_{CH3}$ (ppm)
Oxz 2	γ CH_3[a]	1.41	1.34	0.07
D-Val 3	γ^1CH_3[b]	1.00	0.96	0.04
D-Val 3	γ^2CH_3[c]	1.10	0.98	0.12
Ile 5	γ CH_3	0.76	0.18	0.58
Ile 5	δ CH_3	0.68	0.37	0.31
Oxz 6	γ CH_3[a]	1.41	1.42	−0.01[d]
D-Val 7	γ^1CH_3[b]	1.00	1.12	−0.12[d]
D-Val 7	γ^2CH_3[c]	1.10	1.15	−0.05[d]

[a,b,c] The chemical shift for CH_3 signal is interchangeable in each value.
[d] The negative $\Delta\delta_{CH3}$ value indicates more down-field shift of CH_3 signal for [Phg]ASC than it for ASC.

methyl group signal. These high-field shifts can be probed to detect the CH/π interactions.[23–25] The ^{1}H NMR spectra for ASC (ca. 5 mM) and [Phg]ASC (ca. 5 mM) were measured in CD_3CN solution at room temperature, and the high-field portions are shown in Figure 5. The respective CH_3 proton signals were assigned as listed in Table 1. The positive $\Delta\delta_{CH3}$ (=$\delta_{CH3(ASC)}-\delta_{CH3([Phg]ASC)}$) value indicates a high-field shift in the CH_3 signal. The $\Delta\delta_{CH3}$ values for six methyl groups (γCH_3-Oxz2, γ^1CH_3-D-Val3, γ^2CH_3-D-Val3, γCH_3-Oxz6, γ^1CH_3-D-Val7 and γ^2CH_3-D-Val7) were very small, while significant $\Delta\delta_{CH3}$ values were observed for Ile5 γCH_3 (0.58 ppm) and Ile5 δCH_3 (0.30 ppm).

In the ROESY experiment for [Phg]ASC, rotating Overhauser effects (ROEs) were observed between γCH_3-Ile5 and the aromatic protons of Phg1 (ArH-Phg1) but were not observed between δCH_3-Ile5 and ArH-Phg1 (Fig. 6). This means that the γCH_3 protons of Ile5 are closer to the aromatic ring of Phg1 than to the δCH_3. These observations indicate that γCH_3 is located at a sensitive position for the ring-current effect and are consistent with the crystal structure. ROE itself shows only the proximity, but in combination with the significant high-field shifts elicited by the ring-current effects, it indicates the potential for CH/π interaction between γCH_3-Ile5 and ArH-Phg1.

3.3. CD spectra measurement

The CD spectra of [Phg]ASC were measured in acetonitrile (CH_3CN) while changing the 2,2,2-trifluoroethanol (TFE) concentrations (Fig. 7 (a)). This solvent system monitored the conformational equilibrium of ASCs based on spectral changes.[10,26–28] The CD spectrum of [Phg]ASC in CH_3CN solution showed a positive cotton effect at about 207 nm and a small negative cotton effect at 255 nm. Addition of TFE led to a decrease in $[\theta]_{207}$ and an increase in $[\theta]255$, and a single isosbestic point was observed at 235 nm. Earlier spectral data for ASC in the same solvent system is shown

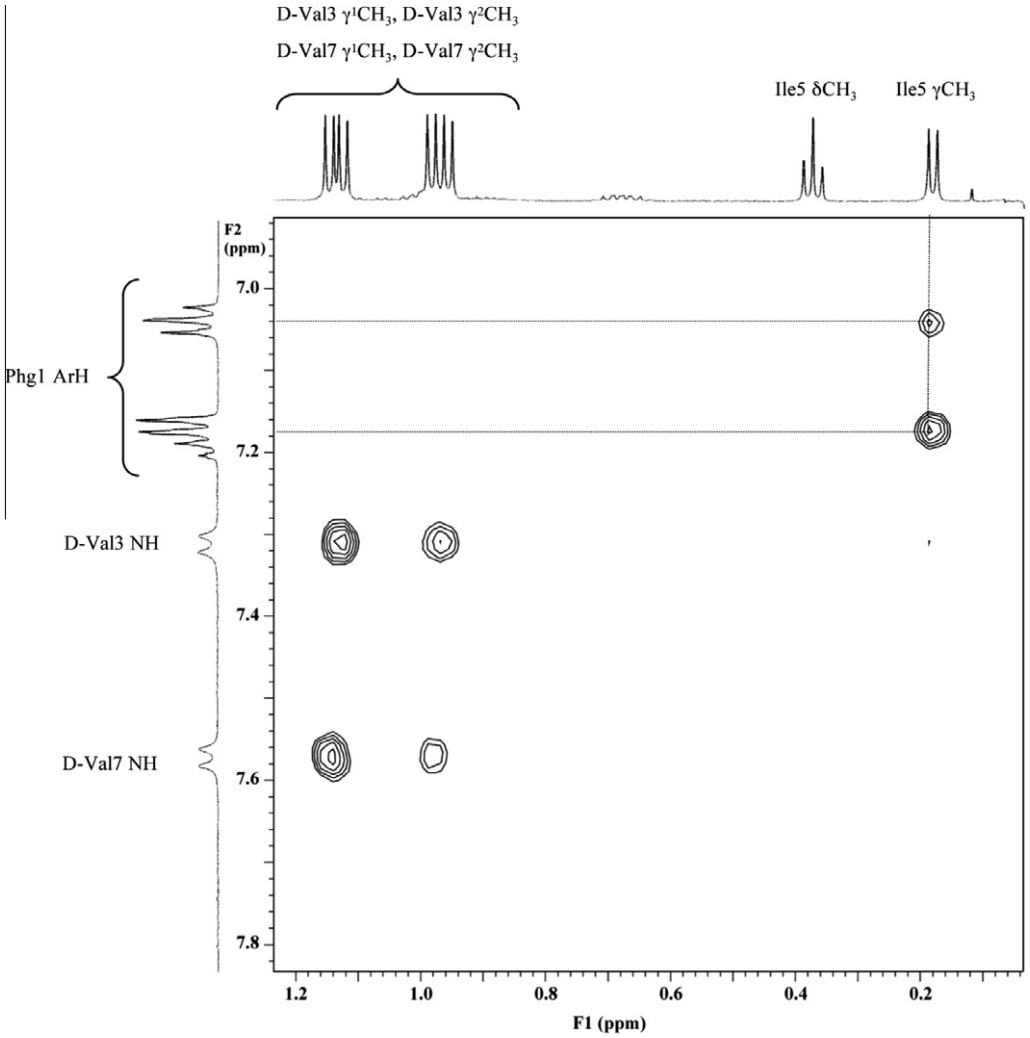

Figure 6. Partial ROESY spectrum for [Phg]ASC in CD_3CN. Each assignment for D-Val3 and D-Val7 are interchangeable.

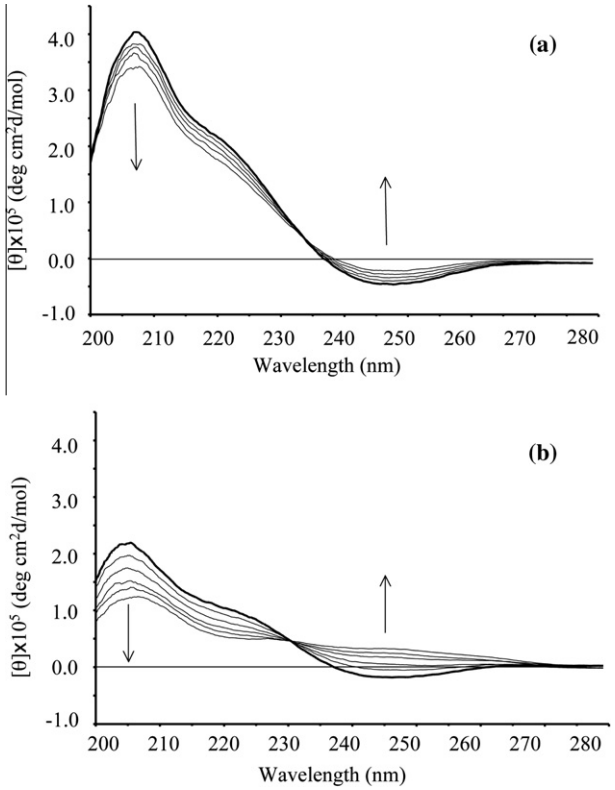

Figure 7. The CD spectra for [Phg]ASC (a) and ASC (b). The CD spectra for ASC is taken from a previous report.[10] The peptide concentrations were approximately 0.04 mmol dm^{-3}. These spectra were measured in CH_3CN solution (bold line) while changing the TFE concentration (10%, 20%, 30%, 40% and 50%).

in Figure 7 (b).[10] We suggest that in the square form, ASC shows a small negative cotton effect at about 255 nm in CH_3CN solution, while the moderate positive cotton effect in the range of 230-260 nm could be a sign of folding. Furthermore, the observed isosbestic point at 230 nm has been suggested that TFE titrations are led to a conformational transformation from the square to the folded form. Thus, the spectral features of [Phg]ASC in this solvent system were similar to those of ASC, but the changes in the [Phg]ASC spectra elicited by TFE titration were smaller than those elicited in the ASC spectra.

We also examined the temperature dependence of the CD spectra of [Phg]ASC in CH_3CN solution at 273-333 K and found that they were little affected by increasing temperature (Fig. 8). Taken

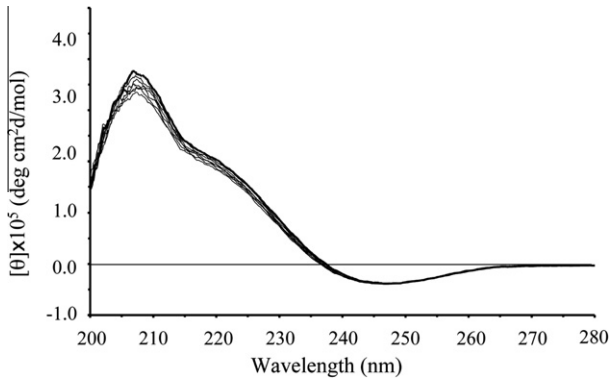

Figure 8. Temperature dependence of CD spectra for [Phg]ASC. The peptide concentrations were approximately 0.04 mmol dm^{-3}. The spectra were measured in CH_3CN solution at 273, 283, 293, 303, 313, 323 and 333 K. The spectrum at 273 K is drawn in bold.

Table 2
The ED_{50} for the cytotoxicity (mg mL^{-1}) of ASC and [Phg]ASC for P388 and HL-60 cells

	P388	HL-60
ASC	10.5[a]	33.5
[Phg]ASC	12.4	12.8

[a] The value is taken from the previous report.[10]

together with the results obtained with TFE, these observations suggest that the square conformation of [Phg]ASC is more stable than that of ASC in CH_3CN solution against the TFE titrations and temperature increases.

3.4. Cytotoxic activity

We assessed the cytotoxicity of [Phg]ASC using P388 mouse lymphocytic leukemia cells and compared them to earlier measurements with ASC.[10] In addition, we also assessed the cytotoxicity of both [Phg]ASC and ASC in HL-60 human myeloblastic leukemia cells. Our findings are summarized in Table 2. The ED_{50} for [Phg]ASC was the same with both P388 and HL-60 cells, whereas the ED_{50} for ASC with HL-60 cells was approximately three times higher than with P388 cells. There is thus good agreement between the cytotoxicity of [Phg]ASC and the square form of ASC; however, [Phg]ASC exhibits greater toxicity toward HL-60 cells than ASC.

4. Conclusion

The square form of [Phg]ASC examined in the present study was similar to that of ASC in crystal. It appears that incorporating the Phg1 residue did not affect the conformation of the peptide backbone, but did affect the molecule's conformational stability. We observed fewer changes in the CD spectra of [Phg]ASC during TFE titration and with increasing temperature than were seen with ASC. ^{1}H NMR analysis of [Phg]ASC revealed significant high-field shifts in the signals for the γCH_3 and δCH_3 of Ile5 due to ring-current effects of the benzene ring of Phg1. In particular, the close proximity of the γCH_3 protons of Ile5 and the aromatic protons of Phg1 were revealed by ROESY measurements and X-ray crystallography. This suggests the potential for CH/π interactions between γCH_3 of Ile5 and the benzene ring of Phg1. In addition, [Phg]ASC showed the stronger cytotoxicity toward HL-60 cells, a human leukemia line, than ASC.

Because the energy of a CH/π hydrogen bond is very weak (2-8 kJ mol^{-1})[29–31], this bond appears to be a less important interaction than the conventional O–H···O= or N–H···O hydrogen bond. However, recent theoretical and experimental studies have shown the importance of weak hydrogen bonds in proteins and peptides.[15,32–36] Thus the presence of CH/π interactions between amino acid side chains within the [Phg]ASC molecule may contribute to its conformational stability.

References and notes

1. Hamamoto, Y.; Endo, M.; Nakagawa, M.; Nakanishi, T.; Mizukawa, K. *Chem. Commun.* **1983**, 323.
2. Ishida, T.; Inoue, M.; Hamada, Y.; Kato, S.; Shioiri, T. *Chem. Commun.* **1987**, 370.
3. Ishida, T.; Tanaka, M.; Nabae, M.; Inoue, M.; Kato, S.; Hamada, Y.; Shioiri, T. *J. Org. Chem.* **1988**, *53*, 107.
4. Ishida, T.; In, Y.; Doi, M.; Inoue, M.; Hamada, Y.; Shioiri, T. *Biopolymers* **1992**, *32*, 131.
5. Schmiz, J. F.; Ksebati, B. M.; Chang, S. J.; Wang, L. J.; Hossain, B. M.; Van Der Helm, D.; Engel, H. M.; Serban, A.; Silfer, A. J. *J. Org. Chem.* **1989**, *54*, 3463.
6. In, Y.; Doi, M.; Inoue, M.; Hamada, Y.; Shioiri, T. *Chem. Pharm. Bull.* **1993**, *41*, 1686.
7. Doi, M.; Shinozaki, F.; In, Y.; Ishida, T.; Yamamoto, D.; Kamigauchi, M.; Sugiura, M.; Hamada, Y.; Kohda, K.; Shioiri, T. *Biopolymers* **1999**, *49*, 459.

8. Asano, A.; Doi, M.; Kobayashi, K.; Arimoto, M.; Ishida, T.; Katsuya, Y.; Mezaki, Y.; Hasegawa, H.; Nakai, M.; Sasaki, M.; Taniguchi, T.; Terashima, A. *Biopolymers* **2001**, *58*, 295.
9. Doi, M.; Asano, A.; Usami, Y.; Katsuya, Y.; Nakai, M.; Sasaki, M.; Taniguchi, T.; Hasegawa, H. *Acta Crystallogr.* **2001**, *E57*, 1019.
10. Asano, A.; Minoura, K.; Yamada, T.; Numata, A.; Ishida, T.; Katsuya, Y.; Mezaki, Y.; Sasaki, M.; Taniguchi, T.; Nakai, M.; Hasegawa, H.; Terashima, A.; Doi, M. *J. Pept. Res.* **2002**, *60*, 10.
11. Hamada, Y.; Kato, S.; Shioiri, T. *Tetrahedron Lett.* **1985**, *26*, 3223.
12. Hamada, Y.; Shibata, M.; Sugiura, T.; Kato, S.; Shioiri, T. *J. Org. Chem.* **1987**, *52*, 1252.
13. Kohda, K.; Ohta, Y.; Yokoyama, Y.; Kato, T.; Suzumura, Y.; Hamada, Y.; Shioiri, T. *Biochem. Pharmacol.* **1989**, *38*, 4497.
14. Kohda, K.; Ohta, Y.; Kawazoe, Y.; Kato, T.; Suzumura, Y.; Hamada, Y.; Shioiri, T. *Biochem. Pharmacol.* **1989**, *38*, 4500.
15. Umezawa, Y.; Tsuboyama, S.; Honda, K.; Uzawa, J.; Nishio, M. *Bull. Chem. Soc. Jpn.* **1998**, *71*, 1207.
16. Takagi, T.; Tanaka, A.; Matsuo, S.; Maezaki, H.; Tani, M.; Fujiwara, H.; Sasaki, Y. *J. Chem. Soc., Perkin Trans. 2* **1987**, 1015.
17. Sakaki, S.; Kato, K.; Miyazaki, T.; Musashi, Y.; Ohkubo, K.; Ihara, H.; Hirayama, C. *J. Chem. Soc., Faraday Trans.* **1993**, *89*, 659.
18. Tsuzuki, S.; Honda, K.; Uchimaru, T.; Mikami, M.; Tanabe, K. *J. Am. Chem. Soc.* **2000**, *122*, 3746.
19. Gung, B. W.; Zhu, Z.; Fouch, R. A. *J. Am. Chem. Soc.* **1995**, *117*, 1783.
20. Fan, M. F.; Lin, Z.; McGrady, J. E.; Mingos, D. M. P. *J. Chem. Soc., Perkin Trans. 2* **1996**, 563.
21. Pauling, L. *The Nature of the Chemical Bonds*; Cornell Univ Press: Ithaca, New York, 1960. p. 260.
22. Rowland, R. S.; Taylor, R. *J. Phys. Chem.* **1996**, *100*, 7384.
23. Kobayashi, K.; Asakawa, Y.; Kikuchi, Y.; Toi, H.; Aoyama, Y. *J. Am. Chem. Soc.* **1993**, *115*, 2648.
24. Maeda, I.; Shimohigashi, Y.; Nakamura, I.; Sakamoto, H.; Kawano, K.; Ohno, M. *Biochem. Biophys. Res. Commun.* **1993**, *193*, 428.
25. Suezawa, H.; Hashimoto, T.; Tsuchinaga, K.; Yoshida, T.; Yuzuri, T.; Sakakibara, K.; Hirota, M.; Nishio, M. *J. Chem. Soc., Perkin Trans. 2* **2000**, 1243.
26. Asano, A.; Yamada, T.; Numata, A.; Katsuya, Y.; Sasaki, M.; Taniguchi, T.; Doi, M. *Biochem. Biophys. Res. Commun.* **2002**, *297*, 143.
27. Asano, A.; Yamada, T.; Numata, A.; Doi, M. *Acta Crystallogr.* **2003**, *C59*, o488.
28. Asano, A.; Yamada, T.; Katsuya, Y.; Taniguchi, T.; Sasaki, M.; Doi, M. *J. Pept. Res.* **2006**, *66*, 90.
29. Nishio, M. *In Encyclopedia of Supramolecular Chemistry*; Marcel Dekker: New York, 2004. 1576.
30. Nishio, M. *CrystEngComm* **2004**, *6*, 130.
31. Nishio, M.; Umezawa, Y.; Honda, K.; Tsuboyama, S.; Suezawa, H. *CrystEngComm* **2009**, *11*, 1757.
32. Umezawa, Y.; Nishio, M. *Bioorg. Med. Chem.* **1998**, *6*, 493.
33. Hatfield, M. P. D.; Palermo, N. Y.; Csontos, J.; Murphy, R. F.; Lovas, S. J. *Phys. Chem. B* **2008**, *112*, 3503.
34. Takahashi, O.; Kohno, Y.; Nishio, M. *Chem. Rev.* **2010**, *110*, 6049.
35. Umezawa, Y.; Tsuboyama, S.; Takahashi, H.; Uzawa, J.; Nishio, M. *Bioorg. Med. Chem.* **1999**, *7*, 2021.
36. Harigai, M.; Kataoka, M.; Imamoto, Y. *J. Am. Chem. Soc.* **2006**, *128*, 10646.